Power-Quality-Oriented Optimization in Multiple Three-Phase Adjustable Speed Drives

Yang, Yongheng; Davari, Pooya; Blaabjerg, Frede; Zare, Firuz

Published in:
Proceedings of the 8th Annual IEEE Energy Conversion Congress and Exposition, ECCE 2016

DOI (link to publication from Publisher):
10.1109/ECCE.2016.7855362

Publication date:
2016

Document Version
Accepted author manuscript, peer reviewed version

Power-Quality-Oriented Optimization in Multiple Three-Phase Adjustable Speed Drives

Yongheng Yang*, *Member, IEEE,* Pooya Davari*, *Member, IEEE,* Frede Blaabjerg*, *Fellow, IEEE* and Firuz Zare†, *Senior Member, IEEE*

*Department of Energy Technology, Aalborg University, Aalborg 9220, Denmark
†Power and Energy Group, The University of Queensland, St. Lucia QLD 4072, Australia
yoy@et.aau.dk; pda@et.aau.dk; fbl@et.aau.dk; f.zare@uq.edu.au

***Abstract*—As an almost standardized configuration, Diode Rectifiers (DRs) and Silicon-Controlled Rectifiers (SCRs) are commonly employed as the front-end topology in three-phase Adjustable Speed Drive (ASD) systems. Features of this ASD configuration include: structural and control simplicity, small volume, low cost, and high reliability during operation. Yet, DRs and SCRs bring harmonic distortions in the mains and thus lowering the overall efficiency. Power quality standards/rules are thus released. For multiple ASD systems, certain harmonics of the total grid current can be mitigated by phase-shifting the currents drawn by SCR-fed drives, and thus it is much flexible to reduce the Total Harmonic Distortion (THD) level in such applications. However, the effectiveness of this harmonic mitigation scheme for multiple ASD systems depends on: a) the number of parallel drives, b) the power levels, and c) the phase-shifts (i.e., firing angles) for the corresponding SCR-fed drives. This paper thus adopts a particle swarm optimization algorithm to optimize the power levels and the firing angles for multi-drive systems considering a fixed number of drives when practically implemented. The optimization is done to minimize the THD level of the total current at the point of common coupling. Simulations with the optimized results are carried out and laboratory tests on a two-drive system are provided to demonstrate the phase-shifting harmonic mitigation scheme. Issues concerning the practical implementation of the optimal results in multi-drive systems are also addressed.**

***Index Terms*—Power quality, harmonics, particle swarm optimization, phase-shifted current control, Diode Rectifiers (DR), Silicon-Controlled Rectifiers (SCR), three-phase Adjustable Speed Drives (ASD).**

I. Introduction

Many industrial applications are using one or more Adjustable Speed Drives (ASDs), which typically consist of an ac-dc rectification stage as the front-end, a dc-link (passive or active), and a dc-ac Variable Frequency Converter (VFC), as it is illustrated in Fig. 1. Considering the cost of installation and possible maintenance, "uncontrollable" Diode Rectifiers (DRs) and "phase-controllable" Silicon-Controlled Rectifiers (SCRs) are widely employed as the front-end apparatus [1]–[5]. However, beyond low cost, small volume, super simplicity, and high reliability during operation, the rectification apparatus in the form of DRs or SCRs significantly distort the grid, where the rectifiers are connected to. As a consequence of a poor harmonic related power quality, efficiency drop, overheating of cables and transformers, malfunction and aging

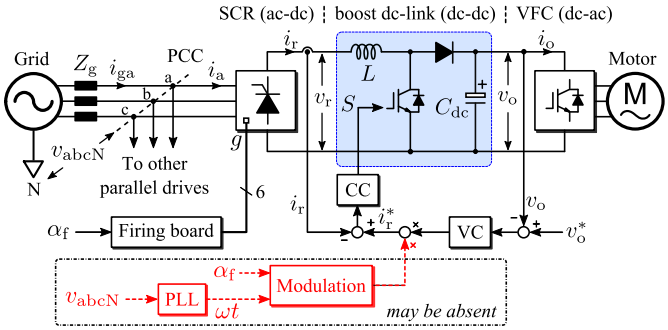

Fig. 1. A silicon controlled rectifier (SCR-fed) ASD system with a boost dc-dc converter in the dc-link (CC - Current Controller; VC - dc-link Voltage Controller; PLL - Phase Locked Loop).

of the electrical equipment connected to the Point of Common Coupling (PCC), triggering system resonance, and in extreme cases a complete power outage, may occur [6], [7]. Thus, the harmonic emission from such drive systems should be limited to an acceptable level defined by system operators (with customers), using:

- Passive filters at the dc-side or ac-side [8]–[10];
- Shunt active power filters [11]–[13];
- Multi-pulse transformer rectifiers [14]–[17]; and
- Hybrid solutions based on the aforementioned (e.g., a combination of passive and active filters) [13], [18]–[20].

Notwithstanding that the current quality is improved, a significant increase in the system volume and/or the control complexity (thus overall cost) has been observed in most of the above solutions. Especially for the multi-pulse transformer rectifiers, the power quality is almost "proportional" to the number of pulses of the transformers, while the overall volume also increases with the number of pulses. At the same time, it is also found that the control flexibility of the harmonics is enhanced when using the active Power Factor Correction (PFC) circuits (or more specifically employing active dc-link circuits) [2], [12], [21]–[24].

Fig. 1 exemplifies a common boost-type PFC three-phase ASD system, where the rectified current (i.e., i_r) can be "controlled (modulated)" as it is highlighted in Fig. 1 and also presented in [21]. The PFCs in three-phase ASD systems

employing DRs and/or SCRs as the front-ends can increase the controllability of the resultant current shapes (and thus the current quality). However, the performance cannot compete with that in single-phase PFC applications [12]. This is due to the inherent behavior of rectifiers in the case of a continuous conduction mode, where ideally the rectifiers draw currents of a rectangular shape with a conduction of 120° [2], [24], [25]. Nevertheless, the configuration in Fig. 1 enables the possibility to shape the currents drawn from the grid with a focus on reducing the distortion level (or mitigating the harmonics of interest, e.g., the 5th- and 7th-order harmonics).

Additionally, in the case of multiple ASDs that are connected to the PCC as shown in Fig. 2, the power quality can be further maximized, since summing up the input currents (i.e., $i_{\rm p1}$, $i_{\rm p2}$, $i_{\rm p3}$, $\cdots$ $i_{\rm pn}$) will result in a mitigation of certain harmonics [6], [7], [21], [26], according to the superposition principle. In that case, the total grid current (i.e., $i_{\rm gp}$ in Fig. 2) will become multilevel, and giving a low THD. Clearly, the number of levels of the resultant grid current depends on the number of drives n, the phase-shift angles to the SCR drives, and the power levels (more specifically, the rectified current levels). As a consequence, the three determining factors should be designed appropriately in such a way that the total grid current (i.e., $i_{\rm gp}$) can be shaped as close as possible to sinusoidal, leading to a high power quality (i.e., low current THD level).

Accordingly, this paper adopts a Particle Swarm Optimization (PSO) [27] algorithm to seek the optimal solution for multiple ASD (n-drive) systems in terms of optimal power levels and firing angles in § III, where the practical implementation issues for the optimized results in multi-drive systems have been addressed as well. The principle of harmonic cancellation by the phase-shifted current control is presented in § II, and it is experimentally demonstrated in § IV on a two-drive system. Simulations on multi-drive systems with the optimization results are also presented, which verifies the discussions - the harmonic mitigation in multi-drive systems has been maximized, leading to an improved current quality. Finally, § V gives concluding remarks on this solution.

II. Phase-Shifted Current Control

The phase-shifted current control method [21], [22], [26] is illustrated in the following on an n-drive system shown in Fig. 2 (n = 2). In practice, the boost PFC is able to regulate the rectified current (e.g., $i_{\rm r1}$) as a purely dc current (denoted as $I_{\rm r1}$) [21], [28], where the boost inductor (i.e., L in Fig. 1) will act like an ideal infinite inductor. In that case, the input currents will be rectangular with a conduction angle of 120°, as previously mentioned and also in [25], [28]. For instance, the phase-a input current of the drive #1 can be given as

$$i_{\rm a1} = \frac{2\sqrt{3}}{\pi} I_{\rm r1} \sum_{h}^{\infty} \left\{ \frac{(-1)^k}{h} \sin\left[h(\omega t - \alpha_{\rm f}\right] \right\} \tag{1}$$

and thus the magnitude of the hth-order harmonic component is obtained as

$$I_{\rm a1}^{h} = \frac{2\sqrt{3}}{\pi h} I_{\rm r1} \tag{2}$$

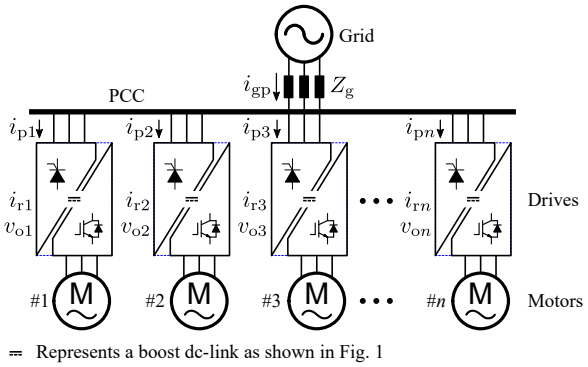

Fig. 2. Layout example of multiple SCR-fed drive systems, where $p = a$, b, or c indicates the corresponding phase and n is the total drive number.

in which $h = 6k \pm 1$ with $h > 0$ being the harmonic order and $k = 0, 1, 2, \cdots$, $\alpha_{\rm f}$ is the firing angle, and $I_{\rm a1}^{h}$ is the magnitude of the hth-order harmonic of the input current $i_{\rm a1}$. According to (1) and (2), a THD level of 31% of the input current $i_{\rm a1}$ is obtained, as it is plotted in Fig. 3(a). When connected to the grid, such a high harmonic distortion level may induce a penalty on the drive system owners.

For multiple SCR-fed drive systems as shown in Fig. 2, certain harmonics can be fully eliminated in theory, as long as the firing angles are properly assigned to specific drive units. This will give an improved power quality, and power-quality related penalties are possible to be avoided as well. Here, the hth-order harmonic phasors (denoted as $\mathbf{I}_{\rm a1}^{h}$ and $\mathbf{I}_{\rm a2}^{h}$) of the considered two-drive system are given as

$$\begin{cases} \mathbf{I}_{\rm a1}^{h} = I_{\rm a1}^{h} e^{j\varphi_{\rm a1}^{h}} \\ \mathbf{I}_{\rm a2}^{h} = I_{\rm a2}^{h} e^{j\varphi_{\rm a2}^{h}} \end{cases} \tag{3}$$

where $I_{\rm a1}^{h}$ and $I_{\rm a2}^{h}$ are the magnitudes, and $\varphi_{\rm a1}^{h}$ and $\varphi_{\rm a2}^{h}$ are the phases of the drive #1 and #2, respectively. The magnitude and phase of the corresponding phasor can be obtained through the Fourier analysis [25] or (1). Then, the hth-order harmonic phasor (denoted as $\mathbf{I}_{\rm ga}^{h}$) of the total grid current $i_{\rm ga}$ can be derived as

$$\mathbf{I}_{\rm ga}^{h} = \mathbf{I}_{\rm a1}^{h} + \mathbf{I}_{\rm a2}^{h} = I_{\rm a1}^{h} e^{j\varphi_{\rm a1}^{h}} + I_{\rm a2}^{h} e^{j\varphi_{\rm a2}^{h}} \tag{4}$$

According to the Cosine Rule, the magnitude of the hth-order harmonic of the grid current can be obtained as

$$I_{\rm ga}^{h} = \left[(I_{\rm a1}^{h})^2 + (I_{\rm a2}^{h})^2 - 2 I_{\rm a1}^{h} I_{\rm a1}^{h} \cos\delta \right]^{1/2} \tag{5}$$

with

$$\delta = \pi - |\varphi_{\rm a1}^{h} - \varphi_{\rm a2}^{h}| \tag{6}$$

in which $|\varphi_{\rm a1}^{h} - \varphi_{\rm a2}^{h}|$ is the phase difference between the two harmonics. Thus, if the hth-order harmonic component of the grid current should be canceled (i.e., $I_{\rm ga}^{h}$ = 0), the two drives have to: a) draw the same level of the harmonic currents from the grid (i.e., $I_{\rm a1}^{h}$ = $I_{\rm a2}^{h}$) and b) have a phase difference of 180° between the two harmonic currents (i.e., δ = 0). Fig. 3 compares the performance of the phase-shifted current control with that in a single drive. It can be seen that the phase-shifted control reduces the distortion level from 31% to 16.4%.

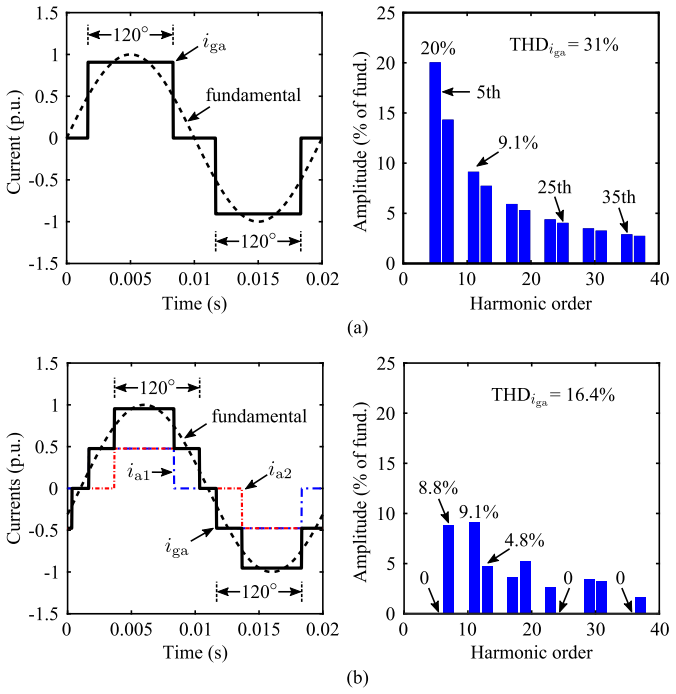

Fig. 3. Harmonic characteristics of the grid current in SCR-fed ASD systems with boost converters in the dc-links (left: ideal waveforms; right: harmonic distribution): (a) a single-drive system with $\alpha_{f1} = 0$ and (b) a two-drive system with $\alpha_{f1} = 0$ and $\alpha_{f2} = 36°$, leading to a cancellation of the harmonics of fivefold the grid fundamental frequency.

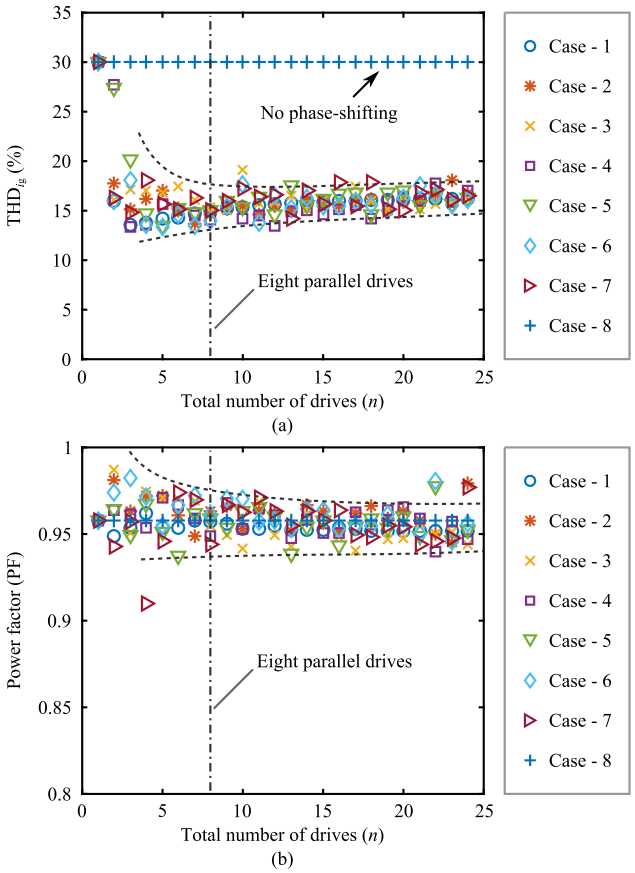

Fig. 4. Performance of a multi-drive system considering parallel drives ($1 \leq n \leq 24$) with the same rated power under random loading conditions: (a) THD level of the total current at PCC and (b) power factor, where the firing angles are linearly assigned (increase) within a range of $0° \leq \alpha_f \leq 30°$. For Case - 1 and Case - 8, the power levels are at the same level among the drives; for Case - 8, the phase-shifting control was not applied.

III. Power-Quality-Oriented Optimization

A. Linear Phase-Shifts for n-Drive Systems

When even more SCR-fed drives are connected to the PCC as shown in Fig. 2, the harmonic mitigation enabled by the phase-shifted current control can be maximized. In that case, the total grid current will have even more levels. This is beneficial to the power quality, when the phase-shifted current control is enabled. Fig. 4 gives numerical simulation results of an n-drive system (up to 24 drives, i.e., $1 \leq n \leq 24$) under random loading conditions, where eight cases have been simulated for the n-drive system. The firing angle for the #k drive is linearly given by

$$\alpha_f^k = (k-1)\frac{\alpha_{fmax}}{n-1} \tag{7}$$

with α_{fmax} being the maximum firing angle. Notably, for Case - 1 and Case - 8, the powers of the SCR-fed drive units are at the same level, and the phase-shifted current control is not activated in Case - 8. In contrast, for the residual tests (Case - 2 to Case - 7), the loading is random with the linearly assigned firing angles according to (7).

It can be observed in Fig. 4 that the THD level of the resultant grid current is around 14-18% and a power factor of around 0.94-0.97 has been achieved, where $0 \leq \alpha_f \leq 30°$. Furthermore, Fig. 4 shows that, when the total number of drives is above eight ($n \geq 8$), both the THD level and the power factor become almost independent of the loading with the linearly designed firing angles [7]. In other words, the THD level and the power factor are bounded within a minor range (around 16%±2% and 0.95±0.02, respectively). Thus, a harmonic mitigation scheme is initiated for multiple ASD systems, where the firing angles can be linearly assigned according to (7).

Additionally, the results imply that considering n drives, there is an optimal operating point in terms of firing angles and power levels, which should ensure a lower THD. For instance, for Case - 7 in Fig. 4, in the case of six parallel drives, a THD of 15% and a power factor of 0.97 have been observed, where the power quality can be further improved by optimizing the firing angles and power levels. This is also demonstrated in a four-SCR-fed system (i.e., $n = 4$ in Fig. 2) with different firing angle strategies but fixed power levels (P_1 = 0.5 kW, P_2 = 2 kW, P_3 = 4 kW, and P_4 = 6 kW). It can be found from the simulation results given in Table I that a THD of 14.1% with the power factor being 0.97 is achieved, when $\alpha_{f1} = 45°$, $\alpha_{f2} = 30°$, $\alpha_{f3} = 15°$, and $\alpha_{f4} = 0°$.

B. Particle Swarm Optimization in n-Drive Systems

Following the above discussions, a Particle Swarm Optimization (PSO) algorithm [27] is adopted to optimize the

TABLE I
CURRENT THD (%) AND POWER FACTOR (PF) FOR THE FOUR-DRIVE SYSTEM WITH DIFFERENT FIRING ANGLES α_{F}.

Firing angle range (°)	$\alpha_{\mathrm{f}} \in$ [0 15]		$\alpha_{\mathrm{f}} \in$ [0 30]		$\alpha_{\mathrm{f}} \in$ [0 45]		$\alpha_{\mathrm{f}} \in$ [0 60]	
	THD_{i_g}	PF	THD_{i_g}	PF	THD_{i_g}	PF	THD_{i_g}	PF
$\alpha_{\mathbf{f}}$ **= linspace(**$\alpha_{\mathbf{fmax}}$**, 0, 4)**	24.2	0.97	18.6	0.97	**14.1**	**0.97**	12.4	0.95
$\alpha_{\mathbf{f}}$ **= linspace(0,** $\alpha_{\mathbf{fmax}}$**, 4)**	24.3	0.95	19.3	0.91	16.4	0.81	16.9	0.64
$\alpha_{\mathbf{f}}$ **= [0.5 2 4 6]**$\times\alpha_{\mathbf{fmax}}$**/12.5**	28.1	0.96	25.4	0.97	22.8	0.97	20.6	0.97

Notes: 1. linspace(x_1, x_2, N) generates N linearly spaced points within [x_1, x_2]; 2. $P_{1,2,3,4}$ = [0.5 2 4 6] kW.

TABLE II
OPTIMIZED RESULTS FOR THE FOUR-DRIVE SYSTEM.

Firing angle range (°)		$\alpha_{\mathrm{f}} \in$ [0 15]	$\alpha_{\mathrm{f}} \in$ [0 30]	$\alpha_{\mathrm{f}} \in$ [0 45]	$\alpha_{\mathrm{f}} \in$ [0 60]
Optimized firing angle $\alpha_{\mathbf{f}}$ **(°)**	α_{f1}	6.4	12.3	38.4	52.4
	α_{f2}	15	18.3	45	60
	α_{f3}	15	30	26.1	39.5
	α_{f4}	0	0	2.1	18
THD$_{i_g}$ **(%)**		20.6	**13.3**	11.2	10.5
Power factor (PF)		0.97	**0.96**	0.94	0.80

multi-drive system with an orientation to seek the optimal operation condition with a high power quality. The optimization objective function is then given as

$$Obj\left(\alpha_{\mathrm{f}j}, P_j\right) = \min_{\{\alpha_{\mathrm{f}j}, P_j\}} \left(\mathrm{THD}_{i_g}\right) \tag{8}$$

with

$$\left[\mathrm{THD}_{i_g}, \mathrm{PF}\right] = f\left(\alpha_{\mathrm{f}j}, P_j, n\right) \tag{9}$$

where $f(\alpha_{\mathrm{f}j}, P_j, n)$ is the numerical harmonic model that is derived from (1) by considering the superposition principle in n-drive systems, P_j is the power for the jth drive with j = 1, 2, 3, ... n, and n is the total drive number. As shown in (9), the numerical harmonic model $f(\alpha_{\mathrm{f}j}, P_j, n)$ is a function of the firing angles, power levels and total drive number, which is in agreement with the previous discussion, and it gives THD_{i_g} and the Power Factor (PF). The optimization outputs are the firing angles α_{f} and/or power levels P of the n-drive system.

Firstly, it is assumed that communication is available in the multi-drive system and the power loading is known and remains unchanged during operation. This means that the optimization variables are only the firing angles, and thus:

$$Obj\left(\alpha_{\mathrm{f}j}\right) = \min_{\alpha_{\mathrm{f}j}} \left(\mathrm{THD}_{i_g}\right) \tag{10}$$

which gives the optimal firing angles that can be dispatched to the multi-drive system in order to minimize the harmonic distortions at the PCC. Again, the previously designed four-SCR-fed drive system is taken into consideration (i.e., the power ratings are P_1 = 0.5 kW, P_2 = 2 kW, P_3 = 4 kW, and P_4 = 6 kW). Applying the PSO algorithm with the objective function in (10) gives the optimization results that are summarized in Table II. Observations in Table II verify that there is an optimal operation point for a multi-drive system with fixed power levels. Specifically, a THD level of 13.3% with a power factor of 0.96 has been achieved for the four-drive system, when the optimization range for the firing angles is $\alpha_{\mathrm{f}} \in$ [0 30]°. At the same time, if the optimization ranges for the firing angles are larger, the THD level can be further reduced at the cost of a lower power factor, as shown in Table II. Therefore, a trade-off between the current quality and PF has to be made in the optimization as well as the design and planning phases of an n-drive system.

However, the drive units of an n-drive (ASD) system are rarely operating at the same power level in practice, and it is also difficult to do online optimization even when the loading information is available. Hence, it is necessary to consider all the determining factors as aforementioned (i.e., number of drives, power levels, and firing angles) in the PSO process (i.e., as variables included in the optimization objective function). In that case, the optimized results will have more degrees of freedom in implementation, which will be elaborated in the next section. Nevertheless, when considering both power levels and firing angles of an n-drive system into the optimization, the objective function in (8) is employed, where the objective is to minimize the THD level. The results are shown in Fig. 5, where it can be observed that the firing angle range and power levels affect the optimization results compared to those in Fig. 4 and Table II. Specifically, a wide range of firing angles (e.g., $0 \leq \alpha_{\mathrm{f}} \leq 45°$) can contribute to an even lower THD level, which can approach to 6%, and the optimal THD level tends to be constant. Furthermore, observations from Fig. 5(b) indicate that a wide range of firing angles may lead to a poor PF after the optimization (e.g., PF = 0.92 in the case of four drives). Considering the PF shown in Fig. 5(b), the firing angle range can be selected as $0 \leq \alpha_{\mathrm{f}} \leq 30°$, where in most cases the power factor is yet around 0.95.

In fact, the PF can be also included into the optimization objective in order to avoid poor power factors when a wide

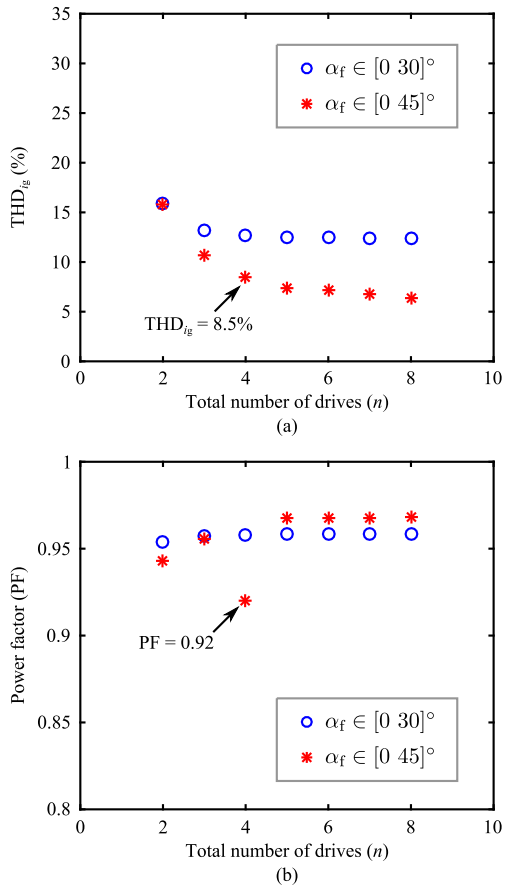

Fig. 5. Optimized results of multi-drive systems considering the firing angles and power levels: (a) THD and (b) power factor.

range of firing angles (e.g., $0 \leq \alpha_f \leq 45°$) is employed. One optimization objective function can be expressed as

$$Obj\,(\alpha_{fj}, P_j) = \min_{\{\alpha_{fj}, P_j\}} \left[\text{THD}_{i_g} \cdot (0.95 - \text{PF})^2 \cdot \gamma\right] \quad (11)$$

which should ensure a PF around 0.95 and also a low THD. In (11), γ is a factor that is used to adjust the optimization convergence speed. A smaller γ may accelerate the optimization, but possibly leading to a poor PF and/or a high THD. Fig. 6 shows an optimized four-drive system in terms of power levels and firing angles, where the objective function shown in (11) is adopted with γ = 1000 and $\alpha_f \in [0\ 45]°$. Compared to the optimization in Fig. 5, it can be seen that the PF has been brought back to around 0.95, since the PF is also included in the optimization objective function of (11). However, it is also observed that the resultant THD level has been slightly increased by 1%. This can be alleviated by further redesigning the objective function as well as the optimization algorithm. Nevertheless, the power quality has been improved in contrast to the results shown in Figs. 3 and 4.

C. Implementation Schemes

As mentioned previously, when a number of drives are considered, online optimization will consume large memory space and computational efforts in the controllers. Furthermore, it will also take much time to update according to instantaneous power loading. Thus, it is more feasible to offline implement the optimal results by means of look-up tables.

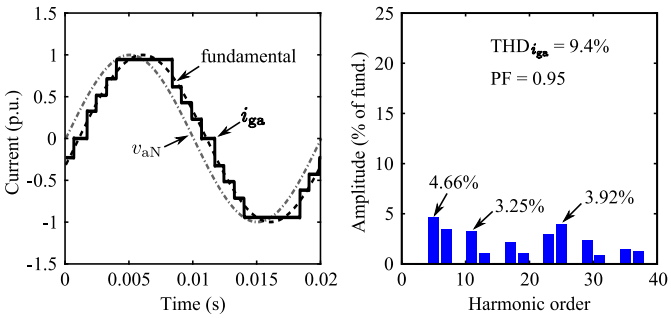

Fig. 6. Example of an optimized 4-drive system in terms of power levels (P_j = [52.9% 56.8% 100% 54.1%] of the rated - 7.5 kW) and firing angles (α_{fj} = [41.28 12.78 0 27.47]°): (a) ideal voltage v_{aN} and the optimized current shape i_{ga} and (b) harmonic distribution of the resultant grid current.

When the total number of drives is above a certain value (e.g., $n \geq 4$), optimizing the firing angles and power levels for all drives is of less meaningfulness, since the power levels will insignificantly affect the optimization results. Hence, an optimization is done first only by considering a limited number of drives (i.e., n = 4), which gives the optimal firing angles and power levels. Following, considering a multi-drive system that has more than four SCR-fed ASDs, the drives can be grouped according to the optimal power levels. Finally, applying the optimal firing angles the corresponding groups leads to the desired optimal current quality at the PCC. Clearly, the more drives the system consists of, the more flexible the grouping can be (i.e., more easier to reach the optimal point).

Furthermore, the optimal grid current shape, which is the summation of the optimized rectangular currents can be programmed into controllers with less computational efforts. In that case, a linear interpolation concept can be adopted to implement the optimized firing angles according to the optimized power levels. Taking an n-drive system as an example and also considering a balanced grid voltage, the optimized current levels (i.e., the rectified currents) can be obtained as

$$I_{rj}^o = \frac{\pi P_j^o}{3\sqrt{2} V_{LL} \cos \alpha_{fj}^o} \quad (12)$$

where V_{LL} is the line-to-line voltage and P_j^o is the optimized power levels with j = 1, 2, 3, ..., n. It is indicated in (12) that the optimized power levels can be mapped to the optimized firing angles (i.e., $P_j^o \rightarrow \alpha_{fj}^o$). Let $P_j^o < P_k \leq P_{j+1}^o$ and $P_n^o = P_r$ with P_k being the power of the kth motor drive and P_r being the maximum rated power, and then the corresponding firing angle α_{fk} can be obtained by means of a bilinear interpolation as

$$\alpha_{fk} = \frac{P_{j+1}^o - P_k}{P_{j+1}^o - P_j^o} \cdot \alpha_{fj}^o + \frac{P_k - P_j^o}{P_{j+1}^o - P_j^o} \cdot \alpha_{f(j+1)}^o \quad (13)$$

in which j = 1, 2, 3, ..., $n-1$. If $P_k < P_1^o$, $\alpha_{fk} = \alpha_{f1}^o$. Similarly, the more the drives are considered, the closer the firing angle gets to its optimum.

TABLE III
PARAMETERS OF THE SIMULATED AND TESTED MULTI-DRIVE SYSTEMS.

Parameter	Symbol	Value
DC-link inductor	L	2 mH
DC-link capacitor	C_{dc}	470 μF
Grid frequency	f_g	50 Hz
Grid phase voltage (RMS)	v_{abcN}	230 V
Grid impedance	Z_g (L_g, R_g)	0.18 mH, 0.1 Ω
PI controller	k_p, k_i	0.01, 0.1

IV. RESULTS

In order to verify the above analysis, simulations have been conducted referring to Figs. 1 and 2, while the phase-shifted current control has also been tested experimentally on a two-drive system. The two-drive system consists of a DR-fed unit (#1) driving an induction motor through a VFC and a SCR-fed unit (#2) adopting resistors as the load. In both systems, Proportional Integral (PI) controllers have been adopted to control the output voltage v_{o} as v_{o}^* = 700 V and the rectified current i_{r} has been controlled through hysteresis controllers (hysteresis band: 2 A for experiments, 1 A for simulations). The PI controller transfer function is given as

$$G_{\text{PI}}(s) = k_p + k_i \cdot \frac{1}{s}$$

with k_p and k_i being the proportional and integral control gains. System parameters of the multi-drive system as well as the controllers are provided in Table III.

Experiments are carried out, and the results are shown in Fig. 7. It can be observed in Fig. 7 that, when the phase-shifted current control is enabled for the two-drive system (i.e., a firing angle of α_{f} = 36° is introduced to the SCR-fed system), the THD level of the total grid current has been reduced to 16.8% compared to the theoretical THD in the case of a single-drive system (e.g., Fig. 3(a)) while a PF of 0.93 is also achieved. The reason for setting a firing angle of α_{f} = 36° is that the harmonics of fivefold the fundamental grid frequency will be minimized in that case. However, due to the line impedance, the 5th-order harmonic is not completely eliminated, as shown in Fig. 7(b). Nevertheless, the effectiveness of the phase-shifted current control to improve the power quality is verified by the experiments.

Furthermore, with an increase of the drive numbers and the availability of communication, the THD level can be further reduced, where the optimization algorithms can be employed as introduced in § III. This is firstly demonstrated by simulations, where a case of random firing angles for the specific four-drive system is simulated. The results are presented in Fig. 8, where α_{f1} = 3.8°, α_{f2} = 27.3°, α_{f3} = 12.4°, and α_{f4} = 27.2°. Although compared to a single-drive system the distortion level is reduced, the THD of the resultant current is relatively high (i.e., 20.7%) under the random firing angles. Then, the optimal firing angles (see Table II with $\alpha_{\text{f}} \in$ [0 30]°)

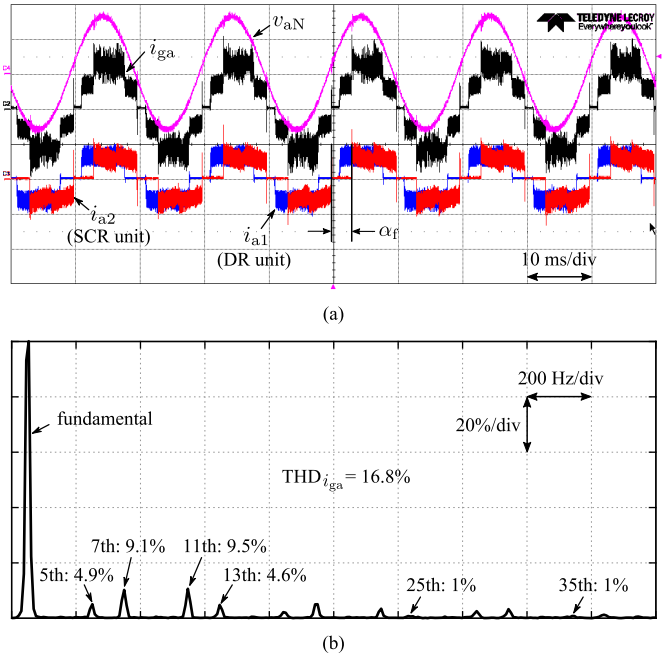

Fig. 7. Experimental results (phase-a) of a two-drive system (a DR-fed and a SCR-fed unit) with the phase-shifted current control (α_{f} = 36°): (a) phase-a currents and voltage (grid voltage v_{aN} [200 V/div], grid current i_{ga} [10 A/div], DR input current i_{a1} [10 A/div], SCR input current i_{a2} [10 A/div]) and (b) Fast Fourier Transform (FFT) analysis of the grid current i_{ga} [% of fundamental], where the total power is 5.92 kW and the PF is 0.93.

are applied to the four-drive system, where a low THD level of 14% and a PF being 0.95 have been achieved, as shown in Fig. 9. The above simulations indicate that, by operating some drives of an n-drive system in partial loading conditions, the current quality can be improved.

However, in practice, it is difficult or even impossible to change the drive loading. Alternatively, the presented optimization results can be programmed according to the implementation schemes in § III.C. By doing so, the firing angles should be optimally dispatched according to the instantaneous loading among the multi-drive system. A dynamic case-study has been conducted on a six-drive system by simulations to demonstrate the implementation scheme, where an optimized four-drive system is adopted, e.g., P_j^o = [71.5% 77.7% 83.7% 100%] of the rated 7.5-kW and $\alpha_{\text{f}j}^o$ = [45 13.4 27.2 0]°, with j = 1, 2, 3, 4. Initially, the power for the six drives are P_k = [6.28 5.48 6.35 7.28 5.94 5.58] kW, and according to the interpolation scheme, the firing angles can be obtained as $\alpha_{\text{f}k}$ = [27.2 36.8 25.5 4.8 16.8 30.1]°, with j = 1, 2, 3, 4, 5, 6. The operating point gives a THD level of 16.2% and a PF of 0.9. At a time instant, the loading is changed to P_k = [7.11 5.49 7.33 7.32 6.94 5.77] kW, and then $\alpha_{\text{f}k}$ = [8.7 36.5 3.8 3.9 12.5 17.2]°, which results in a poorer current quality (i.e., THD: 18.3%) but a PF of 0.95. The high current THD could be reduced to some extent when considering an optimized multi-drive system with more levels. Nevertheless, the simulation results shown in Fig. 10 imply that the optimization results could be implemented based on the bilinear interpolation

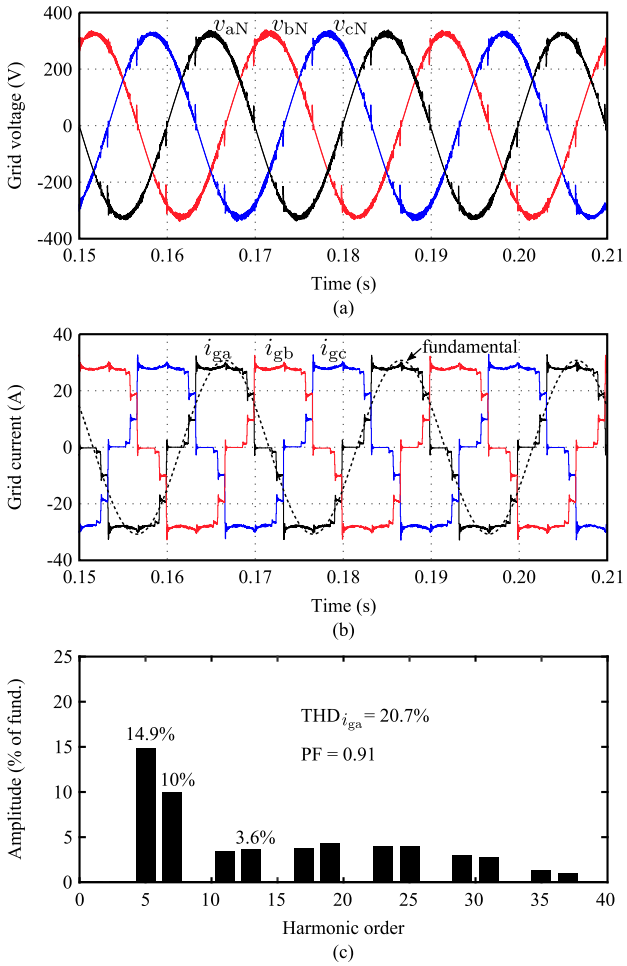

Fig. 8. Simulation results (steady-state) of the four-SCR-fed drive system (P_1 = 0.5 kW, P_2 = 2 kW, P_3 = 4 kW, and P_4 = 6 kW) with random firing angles (i.e., α_{f1} = 3.8°, α_{f2} = 27.3°, α_{f3} = 12.4°, and α_{f4} = 27.2°): (a) grid voltages, (b) total grid currents, and (c) FFT analysis of the phase-a grid current i_{ga}.

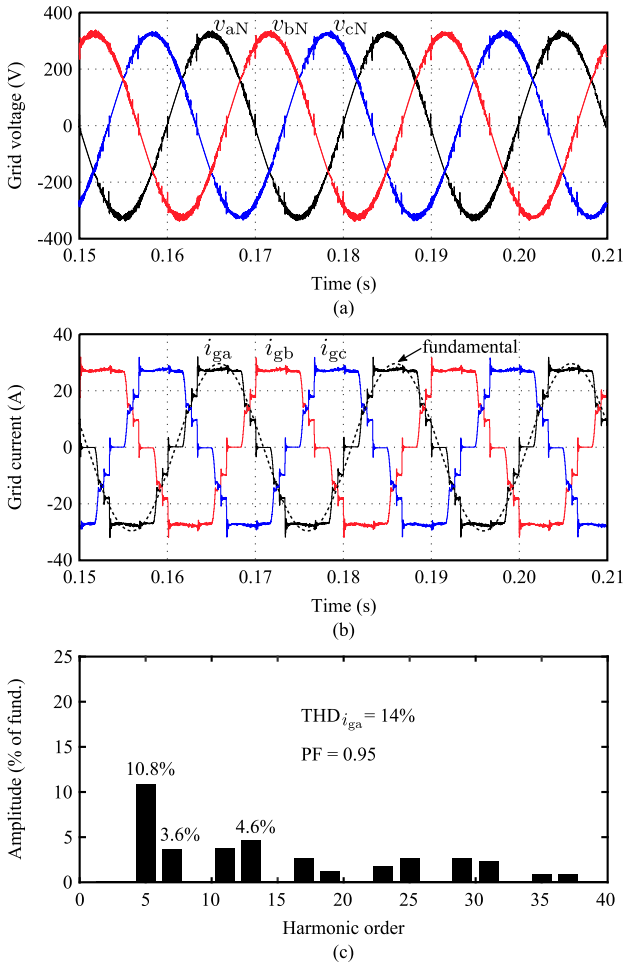

Fig. 9. Simulation results (steady-state) of the four-SCR-fed drive system (P_1 = 0.5 kW, P_2 = 2 kW, P_3 = 4 kW, and P_4 = 6 kW) with optimally dispatched firing angles (i.e., α_{f1} = 12.3°, α_{f2} = 18.3°, α_{f3} = 30°, and α_{f4} = 0°): (a) grid voltages, (b) total grid currents, and (c) FFT analysis of the phase-a grid current i_{ga}.

method, and the multi-drive system can operate smoothly during loading changes. However, how close the resultant power quality is to the optimum depends on the optimized current shape levels as well as the number of drives.

V. Conclusion

In this paper, the harmonic cancellation enabled by mixing multiple ASD systems has been investigated, where the currents drawn by the SCR-fed drives are phase-shifted. This harmonic mitigation scheme has been experimentally demonstrated, where the total grid current (i.e., the current at the PCC) drawn by the rectification apparatus becomes multilevel, leading to an improved power quality. Furthermore, when more drives are connected in parallel, the shape of the total current at the PCC will be much close to sinusoidal, if the firing angles are specifically assigned to the drive systems. It means that there are optimal operation points in terms of power levels and firing angles for these ASD systems, so the THD level can be minimized. Accordingly, an algorithm based on the particle swarm optimization has been adopted with focus to improve the power quality. Simulations performed on three-phase multiple ASD systems with the optimized results have verified the discussions. Considering the practical applications, the implementation of the optimization results involves the knowledge of the power loading among the drives, which requires that communication is available in the system. Look-up table based solutions have also been briefly discussed in this paper, which simplifies the implementation of the optimal results in practical multi-drive systems.

References

[1] P. K. Steimer, "High power electronics innovation," *presented at ICPE - ECCE Asia*, pp. 1–37, Jun. 2015.

[2] J. W. Kolar and T. Friedli, "The essence of three-phase PFC rectifier systems: Part I," *IEEE Trans. Power Electron.*, vol. 28, no. 1, pp. 176–198, Jan. 2013.

[3] P. Barbosa, C. Haederli, P. Wikstroem, M. Kauhanen, J. Tolvanen, and A. Savolainen, "Impact of motor drive on energy efficiency," in *Proc. of PCIM*, pp. 1-6, 2007.

[4] P. Waide and C. U. Brunner, "Energy-efficiency policy opportunities for electric motor-driven systems," *International Energy Agency*, 2011.

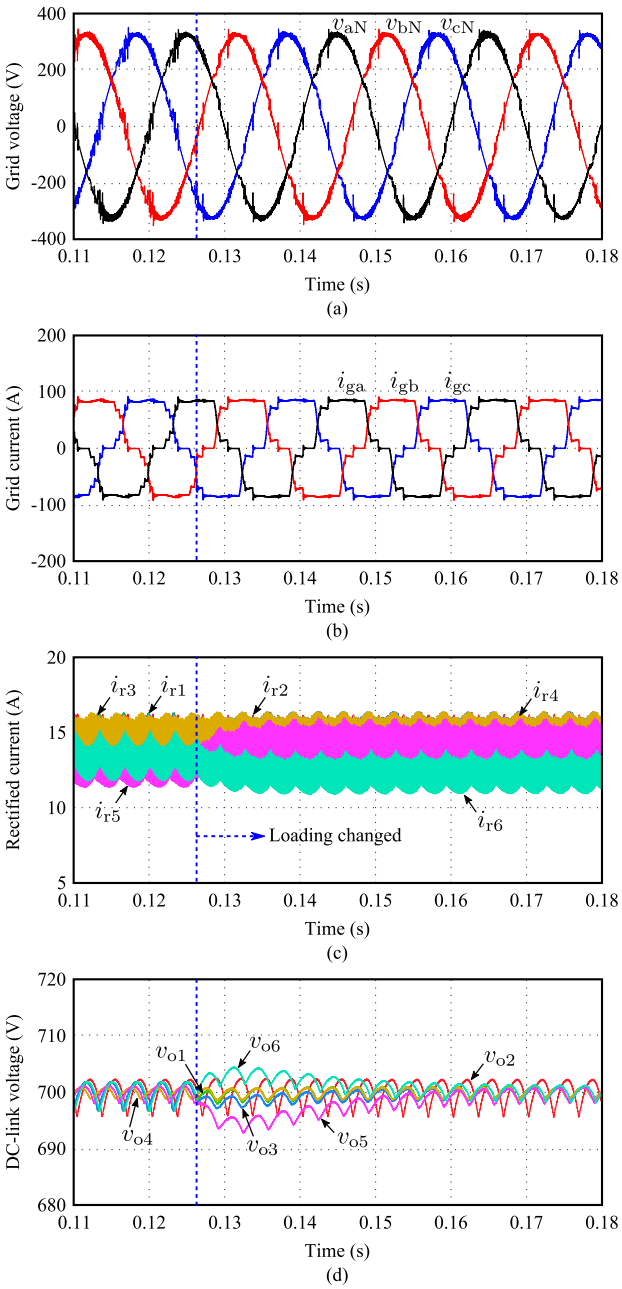

Fig. 10. Simulation results (dynamic) of a six-SCR-fed drive system, where the firing angles have been assigned and implemented according to the interpolation method considering an optimized four-drive system, and the power is changed from P_k = [6.28 5.48 6.35 7.28 5.94 5.58] kW to P_k = [7.11 5.49 7.33 7.32 6.94 5.77] kW: (a) grid voltages, (b) grid currents, (c) rectified currents, and (d) dc-link voltages.

[5] H. Shin, Y. Son, and J. I. Ha, "Grid current shaping method with DC-link shunt compensator for three-phase diode rectifier-fed motor drive system," *IEEE Trans. Power Electron.*, vol. PP, no. 99, pp. 1–10, in press, DOI: 10.1109/TPEL.2016.2540651, 2016.

[6] S. Hansen, P. Nielsen, and F. Blaabjerg, "Harmonic cancellation by mixing nonlinear single-phase and three-phase loads," *IEEE Trans. Ind. Appl.*, vol. 36, no. 1, pp. 152–159, Jan./Feb. 2000.

[7] Y. Yang, P. Davari, F. Zare, and F. Blaabjerg, "Deliberately dispatched SCR firing angles for harmonic mitigation in multiple drive applications without communication," in *Proc. of PEMD*, pp. 1-6, 19-21 Apr. 2016.

[8] H. R. Andersen, R. Tan, and C. Kun, "3-phase AC-drives with passive front-ends with focus on the slim DC-link topology," in *Proc. of PESC*, Jun. 2008, pp. 3248–3254.

[9] S. V. Giannoutsos and S. N. Manias, "A systematic power-quality assessment and harmonic filter design methodology for variable-frequency drive application in marine vessels," *IEEE Trans. Ind. Appl.*, vol. 51, no. 2, pp. 1909–1919, Mar.-Apr. 2015.

[10] K. Lee, D. Carnovale, D. Young, D. Ouellette, and J. Zhou, "System harmonic interaction between DC and AC adjustable speed drives and cost effective mitigation," *IEEE Trans. Ind. Appl.*, vol. PP, no. 99, pp. 1–10, in press, DOI: 10.1109/TIA.2016.2562006, 2016.

[11] H. Akagi, "Active harmonic filters," *Proceedings of the IEEE*, vol. 93, no. 12, pp. 2128–2141, Dec. 2005.

[12] W. J. Lee, Y. Son, and J. I. Ha, "Single-phase active power filtering method using diode-rectifier-fed motor drive," *IEEE Trans. Ind. Appl.*, vol. 51, no. 3, pp. 2227–2236, May-Jun. 2015.

[13] S. Rahmani, A. Hamadi, K. Al-Haddad, and L. A. Dessaint, "A combination of shunt hybrid power filter and thyristor-controlled reactor for power quality," *IEEE Trans. Ind. Electron.*, vol. 61, no. 5, pp. 2152–2164, May 2014.

[14] S. Choi, P.N. Enjeti, and I.J. Pitel, "Polyphase transformer arrangements with reduced kVA capacities for harmonic current reduction in rectifier-type utility interface," *IEEE Trans. Power Electron.*, vol. 11, no. 5, pp. 680–690, Sept. 1996.

[15] M. M. Swamy, "An electronically isolated 12-pulse autotransformer rectification scheme to improve input power factor and lower harmonic distortion in variable-frequency drives," *IEEE Trans. Ind. Appl.*, vol. 51, no. 5, pp. 3986–3994, Sept.-Oct. 2015.

[16] B. Singh, V. Garg, and G. Bhuvaneswari, "A novel T-connected autotransformer-based 18-pulse AC-DC converter for harmonic mitigation in adjustable-speed induction-motor drives," *IEEE Trans. Ind. Electron.*, vol. 54, no. 5, pp. 2500–2511, Oct. 2007.

[17] S. Chiniforoosh, H. Atighechi, and J. Jatskevich, "A generalized methodology for dynamic average modeling of high-pulse-count rectifiers in transient simulation programs," *IEEE Trans. Energy Conversion*, vol. 31, no. 1, pp. 228–239, Mar. 2016.

[18] M. Rastogi, N. Mohan, and A. Edris, "Hybrid-active filtering of harmonic currents in power systems," *IEEE Trans. Power Delivery*, vol. 10, no. 4, pp. 1994–2000, Oct. 1995.

[19] W. Tangtheerajaroonwong, T. Hatada, K. Wada, and H. Akagi, "Design and performance of a transformerless shunt hybrid filter integrated into a three-phase diode rectifier," *IEEE Trans. Power Electron.*, vol. 22, no. 5, pp. 1882–1889, Sept. 2007.

[20] H. Akagi and R. Kondo, "A transformerless hybrid active filter using a three-level pulsewidth modulation (PWM) converter for a medium-voltage motor drive," *IEEE Trans. Power Electron.*, vol. 25, no. 6, pp. 1365–1374, Jun. 2010.

[21] Y. Yang, P. Davari, F. Zare, and F. Blaabjerg, "A DC-link modulation scheme with phase-shifted current control for harmonic cancellations in multidrive applications," *IEEE Trans. Power Electron.*, vol. 31, no. 3, pp. 1837–1840, Mar. 2016.

[22] P. Davari, Y. Yang, F. Zare, and F. Blaabjerg, "A multi-pulse pattern modulation scheme for harmonic mitigation in three-phase multi-motor drives," *IEEE J. Emerg. Sel. Top. Power Electron.*, vol. 4, no. 1, pp. 174–185, Mar. 2016.

[23] T. Friedli, M. Hartmann, and J. W. Kolar, "The essence of three-phase PFC rectifier systems: Part II," *IEEE Trans. Power Electron.*, vol. 29, no. 2, pp. 543–560, Feb. 2014.

[24] H. Y. Kanaan and K. Al-Haddad, "Three-phase current-injection rectifiers: Competitive topologies for power factor correction," *IEEE Ind. Electron. Mag.*, vol. 6, no. 3, pp. 24–40, Sept. 2012.

[25] N. Mohan, T.M. Undeland, and W.P. Robbins, *Power electronics: converters, applications, and design*, 3rd ed. John Wiley & Sons, Inc., Chapter 6 (pp. 138-147), 2007.

[26] E. P. Wiechmann, R. P. Burgos, and J. R. Rodriguez, "Active front-end optimization using six-pulse rectifiers in multi-motor AC drives applications," in *Proc. of IEEE IAS Annual Meeting*, vol. 2, pp. 1294-1299, Oct. 1998.

[27] MathWorks Inc., *Global optimization toolbox: User's guide*, R2015a, Mar. 2015.

[28] H. Ertl and J. W. Kolar, "A constant output current three-phase diode bridge rectifier employing a novel 'Electronic Smoothing Inductor'," *IEEE Trans. Ind. Electron.*, vol. 52, no. 2, pp. 454–461, Apr. 2005.